

Jason C. Brunner \*

Cooperative Institute for Meteorological Satellite Studies (CIMSS)/University of Wisconsin, Madison,  
Wisconsin

Steven A. Ackerman

CIMSS/University of Wisconsin, Madison, Wisconsin

A. Scott Bachmeier

CIMSS/University of Wisconsin, Madison, Wisconsin

Robert M. Rabin

National Oceanic and Atmospheric Administration (NOAA)/National Severe Storm Laboratory (NSSL),  
Norman, Oklahoma

## 1. INTRODUCTION AND BACKGROUND

Researchers have looked at enhanced-V features with 4 km spatial resolution Geostationary Operational Environmental Satellite (GOES) imagery. This paper focuses on observing enhanced-V features with higher (1 km) spatial resolution Polar Orbiting Environmental Satellite (POES) imagery, which has yet to be explored in detail. A quantitative analysis of the enhanced-V feature along with geographic and daytime versus nighttime distributions of enhanced-Vs are presented in this paper.

Many studies have observed and analyzed the enhanced-V feature (McCann 1983; Negri 1982; Heymsfield et al. 1983a, 1983b; Heymsfield and Blackmer 1988; Adler et al. 1985). Enhanced longwave InfraRed (IR) satellite imagery of deep convection sometimes display this cloud-top V-shaped feature, in which an equivalent blackbody temperature (BT) region of a storm is enclosed by a V-shaped region of colder BT (see figure 1a; Negri 1982; McCann 1983; Heymsfield et al. 1983a, 1983b; Fujita 1982). The enhanced-V develops when a strong updraft penetrates into the lower stratosphere and results in an overshooting thunderstorm top. This overshooting top acts to block strong upper level winds and forces the flow to divert around it (Fujita 1978). As the flow is diverted around the overshooting top, it erodes the updraft summit and carries cloud debris downwind (McCann 1983). The carrying of cloud debris downwind is reflected in the colder BTs of the enhanced-V feature (McCann 1983). The coldest BT, which is near

the apex of the enhanced-V, is associated with adiabatic expansion due to the ascent of air parcels in the thunderstorm updraft region overshooting the tropopause (Heymsfield and Blackmer 1988; Adler and Mack 1986).

Several theories have been proposed to explain the warm region of BTs enclosed by the V-feature. One theory argues that the region is a result of subsidence of negatively buoyant overshooting cloud air downstream of an ascending cloud top (Heymsfield and Blackmer 1988; Adler and Mack 1986; Heymsfield et al., 1983a; Negri 1982; Schlesinger 1984). A second theory has been proposed which explains the warm region on the basis of radiative properties of the cloud particles. Based on radiative transfer simulations and assuming that the ice water content varied spatially across the anvil, Heymsfield et al., (1983b) suggested that the interior warm region was found to have lower ice water content compared to the V-arms. This situation implies a smaller optical depth in the warm region and warmer BTs that are characteristic of lower altitudes. Another theory states that stratospheric cirrus (Fujita 1982) generated in the wake of overshooting tops are sinking into the anvil cloud. Located above an anvil top and at a warmer environmental temperature, the stratospheric cirrus appears warmer in the BTs sensed by the IR satellite channel (Wang et al., 2002; Setvak et al., 2005).

Warm regions have been identified as Closed-in Warm Areas (CWA) and Distant Warm Areas (DWA) further downwind (Heymsfield et al., 1983a). The CWA and coldest point of the enhanced-V form a cold-warm couplet (McCann 1983; Heymsfield et al., 1983a, 1983b; Negri 1982; Fujita 1982). A DWA is more transient and usually has no distinct maxima of BT

---

*Corresponding author address:* Jason C. Brunner,  
University of Wisconsin, CIMSS, Madison, WI  
53706; e-mail: [jasonb@ssec.wisc.edu](mailto:jasonb@ssec.wisc.edu).

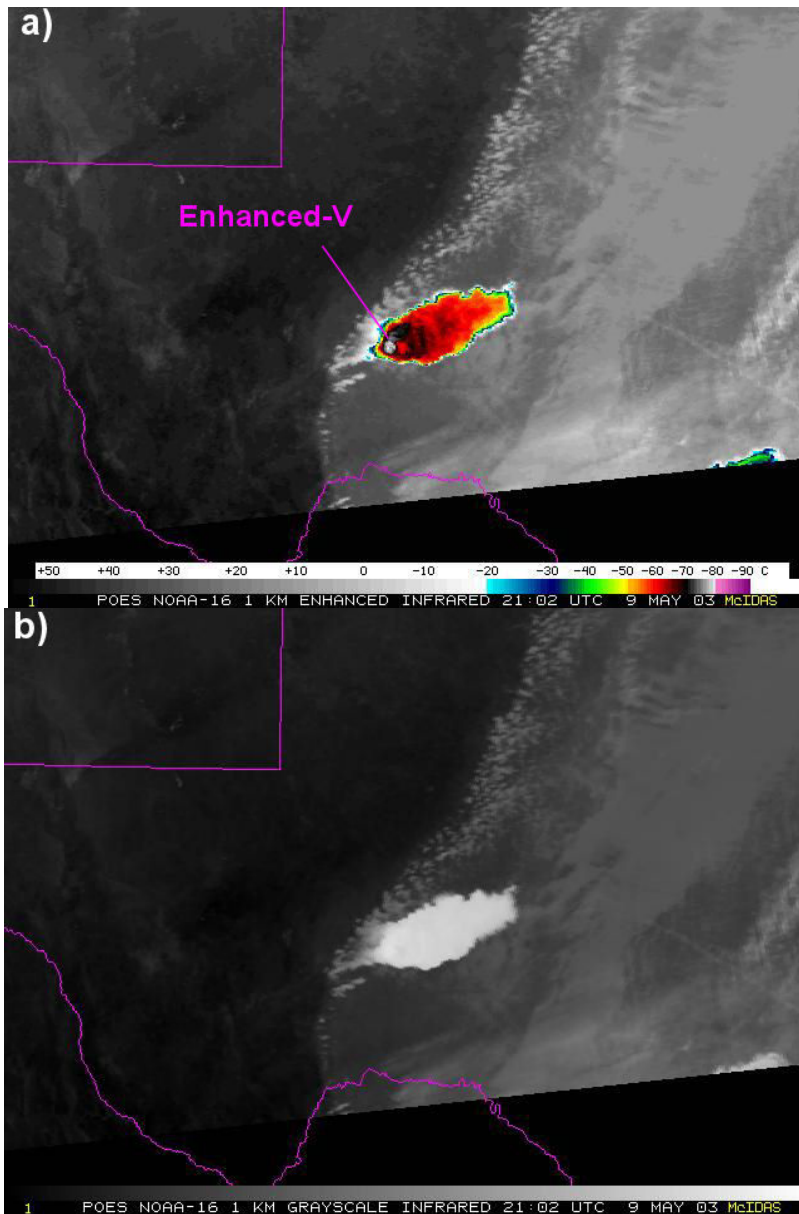


**FIGURE 1.** Deep convective storm with enhanced-V over southwestern Texas from the Polar Orbiting Environmental Satellite (POES) National Oceanic and Atmospheric Administration (NOAA) –Advanced Very High Resolution Radiometer (AVHRR) one-kilometer spatial resolution 10.8  $\mu\text{m}$  IR channel image on 9 May 2003 at 2102 UTC. (a) Color enhanced image (b) Black and white image.

(Heymsfield et al., 1983a). Five Severe Environmental Storms and Mesoscale Experiment (SESAME) cases were performed during 1979 for a GOES quantitative study of the enhanced-V (Heymsfield and Blackmer, 1988). They found that the cold-warm couplet ranged from 7 to 17° C. The distance from the cold point to the CWA was 21 to 44 km and the distance from the cold point to the DWA was 40 to 120 km. Compared to the

CWA, the DWA occurred less frequently and consisted of a larger transient area when present.

The presence of enhanced-V features signifies strong tropospheric shear and intense updrafts, both of which are also essential for severe thunderstorms (Heymsfield and Blackmer 1988). The presence of enhanced-Vs is associated with severe weather (McCann 1983; Negri 1982; Heymsfield et al., 1983a, 1983b; Adler

et al., 1985; Heymsfield and Blackmer 1988). McCann (1983) explored the association of enhanced-Vs to severe weather reports, suggesting their possible use in issuing severe weather warnings. McCann (1983) found a 30-minute median lead time from the time the enhanced-V appeared in enhanced IR imagery to the time of the first report of severe weather. In addition, McCann (1983) found that most of the enhanced-Vs he studied were associated with severe weather (i.e., low false alarm ratio). However, a large number of severe storms did *not* have an enhanced-V (low probability of detection).

Most of these earlier studies of enhanced-V features and their relation to severe weather have used GOES IR imagery with 8 km spatial resolution and 30-minute temporal resolution. The current GOES IR imagery has a spatial resolution of 4 km and improved temporal resolution. POES IR imagery has a spatial resolution of 1 km but with limited temporal resolution as compared to GOES imagery. A few studies have utilized POES IR imagery to investigate enhanced-V features (Adler et al., 1983). Primarily because of the coarse spatial resolution, GOES IR imagery overestimates the cold area BTs by about +15 K for mature thunderstorms and +30-40 K for small growing storms compared to POES IR imagery (Adler et al., 1983). The magnitude of the cold-warm couplet increases dramatically with POES imagery, making it easier to detect. Thus, it is expected that the number of detectable enhanced-Vs will be greater with POES imagery. To date, there has not been a detailed POES dataset of enhanced-V cases developed. This paper explores quantifiable parameters of the enhanced-V and discusses geographic and daytime versus nighttime distributions of the enhanced-V by using a POES dataset.

Section 2 discusses the data used in this study, while Section 3 describes the methodology. Section 4 includes results including quantitative parameters of the enhanced-Vs and geographic and daytime versus nighttime satellite overpass distributions. Conclusions are discussed in Section 5.

## 2. DATA

Two polar orbiting satellite datasets that included the 10.7, 10.8, and 11  $\mu\text{m}$  InfraRed (IR) channels were obtained over the United States of America (USA) for the enhanced-V study. These datasets consisted of:

- POES National Oceanic and Atmospheric Administration (NOAA)-Advanced Very High Resolution Radiometer (AVHRR) and Earth Observing System's (EOS) MODerate-resolution Imaging Spectroradiometer (MODIS) AQUA and TERRA overpasses from 4 May 2003 to 5 July 2003. There were 209 enhanced-V cases collected in the 2003 season.

- POES NOAA-AVHRR and EOS MODIS AQUA and TERRA overpasses from 1 May 2004 to 1 July 2004. There were 241 enhanced-V cases collected in the 2004 season.

In addition, GOES Water Vapor Derived Winds (WVDW) were used to estimate upper tropospheric winds. Archived RADiosonde OBServations (RAOBS) were used if the GOES WVDW were not available at or near the time of the enhanced-V cases.

## 3. METHODOLOGY

### 3.1 Enhanced-V in Satellite Observations

One of the goals of this enhanced-V study is to quantify aspects of the enhanced-V feature using POES observations from the AVHRR and MODIS. These satellites provide a one-kilometer spatial resolution for the 10.8 and 11  $\mu\text{m}$  IR channels. The Man computer Interactive Data Access System (McIDAS) was used to display and analyze the satellite imagery.

As mentioned in the data section, 209 enhanced-V cases were collected from 4 May 2003 to 5 July 2003 and 241 enhanced-V cases were collected from 1 May 2004 to 1 July 2004. Since each polar orbiting satellite has one ascending and one descending overpass per day at a certain location on Earth, the temporal nature of enhanced-V features is difficult to determine. Furthermore, enhanced-V features are associated with deep convection, which usually lasts approximately a few hours. This makes enhanced-V features even more difficult to detect with polar orbiting satellites because of the "hit or miss" nature of the satellite overpasses.

For easy detection of the enhanced-V, the IR imagery is enhanced using the two-ramp dog-leg scheme for converting scene temperatures ( $T_{\text{scene}}$ ) into an unsigned 8-bit integer (count) in the range zero to 255 (Clark 1983, Brunner 2004). Refer to Figure 1b for a POES NOAA-AVHRR

one-kilometer spatial resolution 10.8  $\mu\text{m}$  IR channel image of deep convection over southwestern Texas on 9 May 2003 at 2102 UTC. However, an enhanced-V feature is not evident on this black and white image. Refer to Figure 1a for the same 10.8  $\mu\text{m}$  IR channel image that was used in Figure 1b, but with the addition of the two-ramp dog-leg scheme enhancement. An enhanced-V is labeled on the enhanced IR image.

The enhanced-V has seven quantitative parameters as explained in the following paragraphs:

- TMIN
- TMAX
- TDIFF
- DIST
- DISTARMS
- ANGLEARMS
- ORIENTATION

TMIN is the minimum cloud top equivalent blackbody temperature observed from the satellite. TMIN is usually near the apex of the enhanced-V and is associated with adiabatic expansion due to the ascent of air parcels in the thunderstorm updraft region overshooting the tropopause (Heymsfield and Blackmer 1988; Adler and Mack 1986). The Latitude and Longitude for each enhanced-V case is also documented, based on the position of TMIN.

The maximum cloud top BT is TMAX. TMAX is usually observed downwind of TMIN and is enclosed by the V-feature region. Figure 2a shows a zoomed-in image of Figure 1a with TMIN and TMAX labeled. For this enhanced-V case, TMIN and TMAX were observed to have values of 192 K (-81° C) and 212 K (-61° C), respectively.

The difference in cloud top BTs between TMIN and TMAX (TDIFF) forms a cold-warm couplet (McCann 1983; Heymsfield et al., 1983a, 1983b; Negri 1982; Fujita 1982). Another quantitative parameter of the enhanced-V is the distance between TMIN and TMAX (DIST). Figure 2b displays an enhanced-V with TDIFF and DIST applied and labeled. For this case, TDIFF and DIST were observed to have values of 20 K and 7 km, respectively.

A fifth quantitative parameter used in examining the enhanced-V set is the distance of

the V-arms (DISTARMS). The V-arms extend outward in a V-like pattern from an apex point. Usually, the apex point is denoted as TMIN, and the further away from the apex of the "V", the warmer the cloud top BTs. Sometimes, the apex of the "V" is not TMIN, but it is the coldest cloud top BT along the V-arms. DISTARMS was calculated for each enhanced-V by averaging the two V-arm distances together. The distance of each V-arm was calculated by using McIDAS to measure the distance between the apex point and the point on the V-arm where a noticeable increase in the cloud top BT occurred. This noticeable increase varied for each enhanced-V, but was roughly a 10 percent change between the temperature at the apex point and the temperature at the end of the V-arm.

ANGLEARMS is the angle between the two V-arms. Figure 2c shows DISTARMS and ANGLEARMS applied and labeled to an image; DISTARMS and ANGLEARMS were observed to have values of 22.5 km and 72 degrees, respectively.

The final quantitative descriptor, the ORIENTATION parameter, is used to describe the orientation of the enhanced-V. The ORIENTATION parameter makes four 90-degree quadrants. South was denoted as zero, or 360 degrees. Quadrant 1 (Southwest) is the angle from zero to 90 degrees (West). Quadrant 2 (Northwest) is the angle from 90 to 180 degrees (North). Quadrant 3 (Northeast) is the angle from 180 to 270 degrees (East) and Quadrant 4 (Southeast) is the angle from 270 to 360 degrees.

The quadrant(s) that each enhanced-V was assigned to is determined by two criteria. First, the quadrant that contains the highest number of degrees of the enhanced-V is counted. Second, each quadrant that contains 45 degrees or more is counted. A quadrant was not counted more than once for each enhanced-V. Figure 2d shows an example of the quantitative parameter ORIENTATION. For this enhanced-V case, the enhanced-V orientation was determined to be the northeast quadrant because there were 49 degrees of angle present in the northeast quadrant, while only 23 degrees of angle were present in the southeast quadrant.

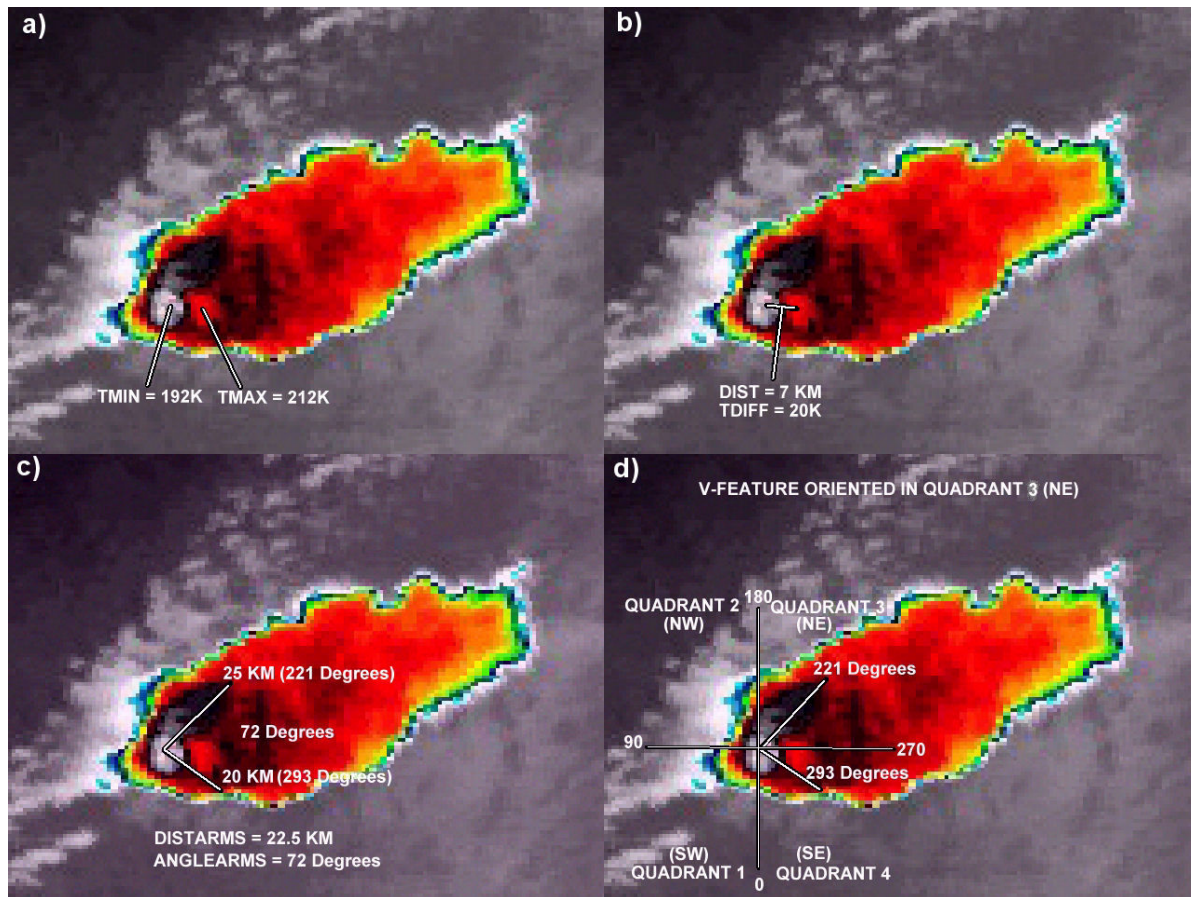


**FIGURE 2.** A zoomed-in POES NOAA-AVHRR one-kilometer spatial resolution enhanced  $10.8 \mu\text{m}$  IR channel image over southwestern Texas on 9 May 2003 at 2102 UTC. The enhanced-V quantitative parameters are labeled in the four panels (a) TMIN (K) and TMAX (K) (b) TDIFF (K) and DIST (KM) (c) DISTARMS (KM) and ANGLEARMS (Degrees), and (d) ORIENTATION.

### 3.2 Upper Level Winds

For the formation of the enhanced-V to occur, it is theorized that strong upper level winds are diverted around the overshooting thunderstorm top (Fujita 1978). In this study, upper level wind speed and direction from the GOES Water Vapor Derived Winds (WVDW) were obtained for each enhanced-V case. The GOES WVDW provide upper level winds every 30 minutes so the temporal resolution is much better than with RAOBS. Also, the horizontal spatial scale is improved with GOES WVDW. If the GOES WVDW were not available at or near the time of an enhanced-V case, then the nearest RAOB both in time and horizontal spatial scale was used instead to determine the upper level winds. For the southwestern Texas enhanced-V case discussed earlier, the upper level wind speed was estimated at 65 Knots (KT) (33 m/s) and the upper level wind direction was towards the northeast.

## 4. RESULTS

This section encompasses two main parts. First, the locations of the enhanced-V cases are included along with a discussion about geographic and daytime versus nighttime satellite overpass distributions of enhanced-Vs. Second, results of the seven enhanced-V quantitative parameters are detailed.

### 4.1 Geographic and Daytime Versus Nighttime Distributions

Figure 3 shows the location of the 450 enhanced-V cases from the 2003 and 2004 seasons. The majority of the enhanced-V cases occurred over the Great Plains and Midwestern parts of the United States. With only a few reports of enhanced-V cases over the northeastern and western parts of the United States, there seems to be a high geographical distribution of enhanced-V cases to the Great Plains and Midwestern climatic

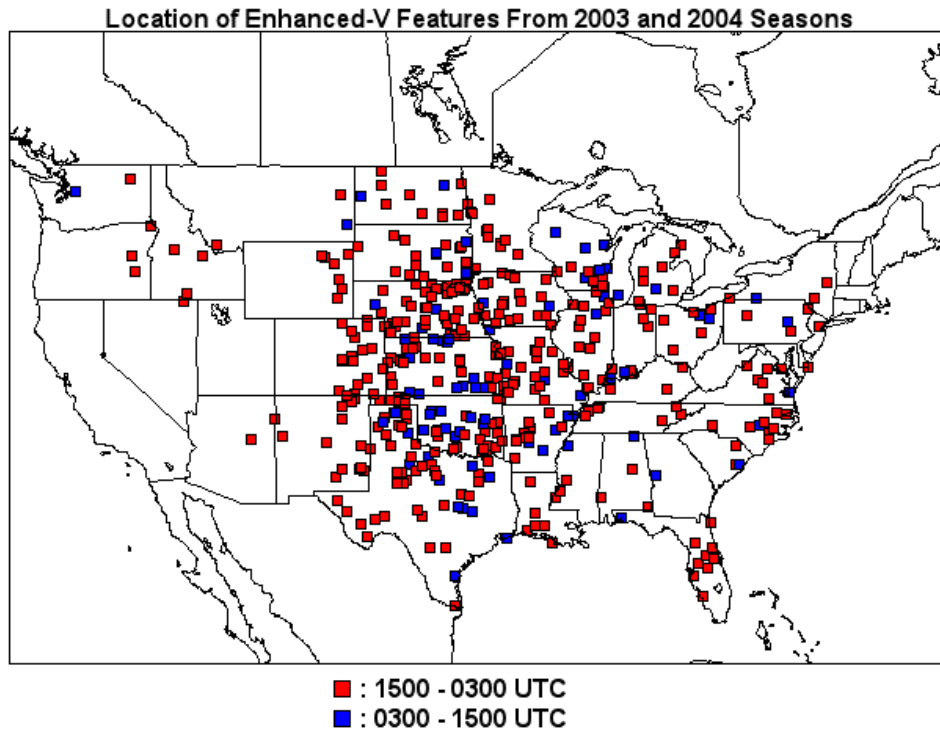


**FIGURE 3:** This map shows the location of the enhanced-V cases over the United States from the 2003 and 2004 seasons. There are a total of 450 enhanced-V cases. Most of the enhanced-V features are located over the Great Plains and Midwestern parts of the United States. The enhanced-V cases that are labeled in red occurred between 1500 and 0300 UTC (daytime and evening hours), while enhanced-V cases that are labeled in blue occurred between 0300 and 1500 UTC (nighttime and morning hours). Overall, a majority of the enhanced-V cases occurred during the afternoon and evening overpasses.

regions. However, since the two seasons include only POES imagery, there may have been enhanced-V features that were not detected, because they occurred before or after the satellite overpass. In addition, the peak frequency for thunderstorms over the northeastern United States is during the month of July (Changnon 2001), so it is possible that there may have been a few more enhanced-V cases detected over the northeast United States if the datasets had included the whole month of July. Our datasets included data from early May to early July. However, the geographic distribution observed in our data is consistent with the distribution in previous studies of enhanced-V features. In past studies, almost every enhanced-V case study occurred over the Great Plains and Midwestern parts of the United States (e.g., Adler et al., 1985; Heymsfield and Blackmer 1988; Heymsfield and Fulton 1994; Heymsfield et al., 1983a, 1983b; McCann 1983; Negri 1982). The geographic distribution of enhanced-Vs is related to the climatology of severe thunderstorms. Compared to the rest of the United States, the Great Plains and Midwest

are climatologically favored for deep convection (Changnon 2001).

In addition to the geographic distribution, there is a noticeable difference in the daytime and nighttime satellite distribution. Figure 3 shows when the enhanced-V features appeared. The enhanced-V cases that occurred between 1500 and 0300 UTC are labeled in red and are considered daytime/evening convection, while enhanced-V cases that occurred between 0300 UTC and 1500 UTC are labeled in blue and are considered nighttime/morning convection. Approximately 81 percent of the total number of enhanced-V cases (366 out of 450 cases) for the two seasons occurred between 1500 and 0300 UTC. This seems reasonable as severe weather (i.e., especially tornadoes) usually occurs during the afternoon and evening hours (Ackerman and Knox, 2003).

#### 4.2 Enhanced-V Parameters

Seven quantitative parameters of the enhanced-V cases were analyzed. Table 1 shows

**TABLE 1.** The Mean, Median, Maximum, and Minimum values for TMIN (K), TMAX (K), TDIFF (K), DIST (KM), DISTARMS (KM), and ANGLEARMS (DEGREES) for the 2003 and 2004 enhanced-V seasons.

<b>2003 SEASON:</b>				
<b>PARAMETER</b>	<b>MEAN</b>	<b>MEDIAN</b>	<b>MAXIMUM</b>	<b>MINIMUM</b>
TMIN (K)	201	200	222	184
TMAX (K)	217	217	246	205
TDIFF (K)	16	16	35	5
DIST (KM)	11	10	43	3
DISTARMS (KM)	39	31	177	9
ANGLEARMS (DEGREES)	78	75	130	25
<b>2004 SEASON:</b>				
<b>PARAMETER</b>	<b>MEAN</b>	<b>MEDIAN</b>	<b>MAXIMUM</b>	<b>MINIMUM</b>
TMIN (K)	201	201	220	181
TMAX (K)	217	217	232	206
TDIFF (K)	16	15	41	5
DIST (KM)	10	9	41	3
DISTARMS (KM)	41	34.5	146.5	10
ANGLEARMS (DEGREES)	75	74	117	38

results from both seasons for the TMIN, TMAX, TDIFF, DIST, DISTARMS, and ANGLEARMS parameters. The Mean (ME), Median (MED), Maximum (MAX), and Minimum (MIN) values of each parameter were calculated. All of the TMIN values were consistent for the 2003 and 2004 seasons. For the TMAX parameter, the MAX value of 246 K (-27° C) in the 2003 season was 14 K larger than the value for the 2004 season. Most of the TDIFF values were consistent for the two seasons except for the MAX value of 41 K for the 2004 season, which was 6 K larger than the MAX value for the 2003 season. All of the DIST values were consistent for the two seasons. Most of the DISTARMS values were consistent for the two seasons except for the MAX value of 177 km for the 2003 season, which was 30.5 km larger than the MAX value for the 2004 season. The ME and MED values for the ANGLEARMS parameter were consistent for the two seasons. However, the MAX and MIN values for the ANGLEARMS parameter were 13 degrees larger and smaller, respectively, for the 2003 season compared to the 2004 season.

The results for the ORIENTATION parameter showed that 59.8 and 72.6 percent of the time an enhanced-V was present in the northeast (number 3) quadrant, for the 2003 and 2004 seasons, respectively. Also, the results showed that 37.8 and 27.8 percent of the time an enhanced-V was present in the southeast (number 4) quadrant, for the 2003 and 2004 seasons, respectively. The northwest (number 2) quadrant

contained enhanced-Vs 9.6 and 2.9 percent of the time for the 2003 and 2004 seasons, respectively; while the southwest (number 1) quadrant contained enhanced-Vs 4.8 and 1.2 percent of the time for the 2003 and 2004 seasons, respectively. The northeast and southeast quadrants contained by far the highest percentages of enhanced-Vs, while the southwest and northwest quadrants had much smaller percentages of enhanced-Vs. For the southwest, northwest, and southeast quadrants, the percent of the time an enhanced-V was present decreased by 3.6 percent, 6.7 percent, and 10 percent, respectively, in the 2004 season compared to the 2003 season. However, for the northeast quadrant, the percent of the time an enhanced-V was present increased by 12.8 percent.

## 5. CONCLUSIONS

The two enhanced-V seasons (early May to early July 2003 and 2004) in this study showed a geographic distribution of enhanced-V features in the Midwest and Great Plains. Only a few enhanced-V features occurred in the western and northeastern parts of the United States of America. There was also a daytime versus nighttime satellite overpass distribution with the enhanced-V features. Most of the enhanced-V features (81 percent) from the two seasons occurred during the afternoon and evening hours rather than the overnight and early morning hours.

The Upper Level Wind Direction and Upper Level Wind Speed can be obtained from the GOES WVDW. These WVDW provide a temporal scale of every half hour compared to Radiosonde Observations (RAOBs), which occur twice per day. Also, the spatial scale is usually better with the WVDW compared to RAOBs. The UL WIND DIR could be used for pattern recognition in an enhanced-V automated detection algorithm. The WVDW could obtain the direction that the enhanced-V is oriented towards and then the algorithm could search for patterns in the equivalent blackbody temperatures.

While the GOES ABI will not have the same spatial resolution as polar orbiting satellite imagery, the two-kilometer spatial resolution will be an improvement from the current four-kilometer GOES satellite imagery and the temporal resolution will be superior to that of polar orbiting satellites. The spatial resolution of polar orbiting satellite imagery and the improved spatial resolution of the upcoming GOES ABI allow a detailed quantitative study of the enhanced-V feature.

*Acknowledgements.* The archived POES NOAA-AVHRR overpasses were obtained from the Satellite Active Archive (SAA) and archived EOS MODIS AQUA and TERRA overpasses were obtained from the Goddard Space Flight Center (GSFC) Distributed Active Archive Center (DAAC). GOES WVDW were provided by Bob Rabin at the Cooperative Institute for Meteorological Satellite Studies (CIMSS) at UW-Madison. These upper level wind speeds and directions were estimated from the automated satellite winds algorithm developed at CIMSS. Archived RAOBS were obtained from the Department of Atmospheric Science at the University of Wyoming.

## REFERENCES

Ackerman, S. A., and J. A. Knox, 2003: *Meteorology: Understanding the Atmosphere*. Brooks/Cole, Pacific Grove, California, Chapter 11.

Adler, R. F., and R. A. Mack, 1986: Thunderstorm cloud top dynamics as inferred from satellite observations and a cloud top parcel model. *Journal of Atmospheric Science*, **43**, 1945-1960.

Adler, R. F., M. J. Markus, and D. D. Fenn, 1985: Detection of severe Midwest thunderstorms using geosynchronous satellite data. *Monthly Weather Review*, **113**, 769-781.

Adler, R. F., M. J. Markus, D. D. Fenn, G. Szejwach, and W. E. Shenk, 1983: Thunderstorm top structure observed by aircraft overflights with an infrared radiometer. *Journal of Applied Meteorology*, **22**, 579-593.

Brunner, J. C., 2004: *A Quantitative Analysis Of The Enhanced-V Feature In Relation To Severe Weather*. M. S. thesis, Dept. of Atmospheric and Oceanic Sciences, University of Wisconsin-Madison, 96 pp.

Changnon, S. A., 2001: *Thunderstorms Across the Nation: An Atlas of Storms, Hail, and Their Damages in the 20<sup>th</sup> Century*. Changnon Climatologist, Mahomet, Illinois.

Clark, J. D. (ed.), 1983: *The GOES User's Guide*. U.S. Dept. of Commerce, Washington D.C.

Fujita, T. T., 1978: Manual of downburst identification for Project NIM-ROD. SMRP 156, University of Chicago, 104 pp.

Fujita, T. T., 1982: Principle of stereoscopic height computations and their applications to stratospheric cirrus over severe thunderstorms. *Journal of Meteorological Society of Japan*, **60**, 355-368.

Heymsfield, G. M., and R. H. Blackmer, Jr., 1988: Satellite-observed characteristics of Midwest severe thunderstorm anvils. *Monthly Weather Review*, **116**, 2200-2224.

Heymsfield, G. M., and R. Fulton, 1994: Passive microwave structure of severe tornadic storms on 16 November 1987. *Mon. Wea. Rev.*, **122**, 2587-2595.

Heymsfield, G. M., R. H. Blackmer, Jr., and S. Schotz, 1983: Upper level structure of Oklahoma tornadic storms on 2 May 1979, Pt. 1 radar and satellite observations. *Journal of Atmospheric Science*, **40**, 1740-1755.

Heymsfield, G. M., G. Szejwach, S. Schotz, and R. H. Blackmer, Jr., 1983: Upper level structure of Oklahoma tornadic storms on 2 May 1979, Pt. 2 Proposed explanation of "V" pattern and internal warm region in infrared observations. *Journal of Atmospheric Science*, **40**, 1756-1767.

Homar, V., M. Gaya, and C. Ramis, 2001: A synoptic and mesoscale diagnosis of a tornado



outbreak in the Balearic Islands. *Atmospheric Research*, **56**, 31-55.

Levizzani, V., and M. Setvak, 1996: Multispectral, high-resolution satellite observations of plumes on top of convective storms. *Journal of Atmospheric Science*, **53**, 361-369.

Mack, R. A., A. F. Hasler, and R. F. Adler, 1983: Thunderstorm cloud top observations using satellite stereoscopy. *Monthly Weather Review*, **111**, 1949-1964.

McCann, D. W., 1983: The enhanced-V: A satellite observable severe storm signature. *Monthly Weather Review*, **111**, 887-894.

Negri, A. J., 1982: Cloud-top structure of tornadic storms on 10 April 1979 from rapid scan and stereo satellite observations. *Bulletin of the American Meteorological Society*, **63**, 1151-1159.

Scanlon, R. J., 1987: *Mesoscale application of high resolution imagery*. M. S. thesis, Dept. of The Navy, Naval Postgraduate School, 133 pp.

Schlesinger, R. E., 1984: Mature thunderstorm cloud-top structure and dynamics: A three-dimensional numerical simulation study. *Journal of Atmospheric Science*, **41**, 1551-1570.

Schlesinger, R. E., 1988: Effects of stratospheric lapse rate on thunderstorm cloud-top structure in a three-dimensional numerical simulation, Pt. 1, Some basic results of comparative experiments. *Journal of Atmospheric Science*, **45**, 1555-1570.

Schmit, T. J., M. M. Gunshor, W. P. Menzel, J. Li, S. Bachmeier, and J. J. Gurka, 2004: Introducing the Next-generation Advanced Baseline Imager (ABI) on Geostationary Operational Environmental Satellites (GOES)-R, Submitted to the *Bulletin of the American Meteorological Society*.

Setvak, M., R. M. Rabin, and P. K. Wang, 2005: Contribution of MODIS instrument to the observations of deep convective storms and stratospheric moisture detection in GOES and MSG imagery. *Atmospheric Research (submitted in March 2005; accepted for press in September 2005)*.

Setvak, M., R. M. Rabin, C. A. Doswell III, and V. Levizzani, 2003: Satellite observations of convective storm tops in the 1.6, 3.7, and 3.9  $\mu\text{m}$

spectral bands. *Atmospheric Research*, **67**, 607-627.

Wang, P. K., H-m. Lin, S. Natali, S. Bachmeier, and R. Rabin, 2002: Cloud model interpretation of the mechanisms responsible for the satellite-observed enhanced V and other features atop some Midwest severe thunderstorms. *Proceedings of the 11<sup>th</sup> American Meteorological Society Conference on Cloud Physics*, Ogden, UT, June 3-7, 2002.